The Mix family homeodomain gene *bonnie and clyde* functions with other components of the Nodal signaling pathway to regulate neural patterning in zebrafish

Le A. Trinh[1], Dirk Meyer[2] and Didier Y. R. Stainier[1,*]

[1]Department of Biochemistry and Biophysics, Programs in Developmental Biology, Genetics and Human Genetics, University of California, San Francisco, San Francisco, CA 94143-0448, USA
[2]Abteilung für Entwicklungsbiologie, Biologie I, Universität Freiburg, Hauptstrasse 1, D-79104 Freiburg, Germany
*Author for correspondence (e-mail: didier_stainier@biochem.ucsf.edu)

Accepted 12 May 2003

Development 130, 4989-4998

doi:10.1242/dev.00614

Summary

Mix family homeodomain proteins, such as *Xenopus* Mixer and zebrafish Bonnie and clyde (Bon), have been shown to regulate the formation of the endoderm and are likely to be transcriptional mediators of Nodal signaling. Here, we show that, in addition to its previously described role in endoderm formation, Bon also regulates the anteroposterior patterning of the neuroectoderm. *bon*-mutant embryos exhibit an anterior reduction of the neural plate. By using targeted injection of antisense morpholino oligonucleotides, we demonstrate that Bon is required in the axial mesoderm for anterior neural development. Consistent with these results, *bon*-mutant embryos show defects in axial mesoderm gene expression starting at mid-gastrulation stages. In addition, genetic analyses demonstrate a functional interaction during neural patterning between *bon* and two components of the Nodal signaling pathway, the *nodal*-related gene *squint* (*sqt*) and *forkhead box H1* [*foxh1*; mutant locus *schmalspur* (*sur*)]. *bon*$^{-/-}$;*sqt*$^{-/-}$ and *bon*$^{-/-}$;*sur*$^{-/-}$ embryos exhibit neural patterning defects that are much more severe than those seen in the single mutants, suggesting that these genes function in parallel in this process. We also show that the severity of the neural patterning defects in the single- and double-mutant embryos correlates with the degree of reduction in expression of the Wnt antagonist gene *dickkopf 1*. Furthermore, *bon*$^{-/-}$;*sqt*$^{-/-}$ and *bon*$^{-/-}$;*sur*$^{-/-}$ embryos exhibit identical morphological and gene expression defects, suggesting, in part, that *bon*, *sqt* and *sur* (*foxh1*) play overlapping roles in neural patterning. Taken together, these results provide evidence for a complex genetic network in which *bon* functions both downstream of, and possibly in parallel to, Nodal signaling to regulate neural patterning via the modulation of mesendodermal gene expression.

Key words: Mix-like, *nodal*, *fast1/foxHI*, Neural patterning, Zebrafish

Introduction

The establishment of cell fates along the anteroposterior (AP) axis of the neural plate is modulated by multiple signaling pathways, including the Wnt, Bmp and Nodal pathways (reviewed by Yamaguchi 2001; Thisse et al., 2000; Erter et al., 2001; Kudoh et al., 2002). The Nodal signaling pathway has been most extensively studied for its role in the formation and patterning of the mesoderm and endoderm (reviewed by Schier and Shen, 1999). Studies in amphibians, mice and zebrafish all point to Nodal ligands as potent inducers of mesodermal and endodermal cell fates (Conlon et al., 1994; Feldman et al., 1998; Sampath et al., 1998; Osada and Wright, 1999). In patterning the neuroectoderm, Nodal signaling has been suggested to specify anterior fates, as mouse chimeras with *Nodal*-mutant cells in the visceral endoderm lack anterior fates (Brennan et al., 2001). In addition, analyses of a hypomorphic *nodal* allele reveal that reduced levels of Nodal function result in anterior patterning defects in mouse (Lowe et al., 2001). However, it is unclear how a reduction in Nodal signaling leads to neural patterning defects.

Nodals belong to the Tgfβ superfamily of ligands that bind to and activate heteromeric type I and type II Activin-like receptors (reviewed by Whitman, 2001). The founding member of this Tgfβ subgroup, mouse Nodal, was identified from studying a retroviral insertion that affects node formation (Zhou et al., 1993). In zebrafish, two *nodal*-related genes, *cyclops* (*cyc*) and *squint* (*sqt*), are required for the induction of the axial and trunk mesoderm, as well as the endoderm (Feldman et al., 1998; Sampath et al., 1998). Nodal signaling also appears to be important for neural patterning, as embryos mutant for both *cyc* and *sqt* appear to have expanded anterior neural fates and loss of trunk spinal cord (Feldman et al., 2000). Additionally, in maternal-zygotic *one-eyed pinhead* (*MZoep*)-mutant embryos, which lack an EGF-CFC cofactor essential for Nodal signaling, anterior fates appear expanded (Gritsman et al., 1999). However, compound mutant analyses of embryos lacking *sqt* and *bozozok* (*boz*), a homeobox gene required for axis formation, indicate that *sqt* acts in parallel with *boz* to specify anterior neuroectoderm, whereas *cyc* represses anterior neural development (Sirotkin et al., 2000).

These data suggest that Nodal signaling can play both positive and negative roles in neuroectoderm patterning, and that the correct balance needs to be achieved for the process to occur correctly.

Loss- and gain-of-function analyses indicate that Nodal signaling is transduced by Smad2 (Madh2 – Zebrafish Information Network), and to some extent Smad3 (Madh3a – Zebrafish Information Network). These receptor-activated Smads are phosphorylated by ligand binding to the receptor complex (Waldrip et al., 1998; Tremblay et al., 2000; Brennan et al., 2001). Mouse *Smad2* mutants, like *Nodal* mutants, exhibit defects in the formation of the primitive streak, mesoderm and endoderm (Waldrip et al., 1998; Weinstein et al., 1998). Interestingly, *Nodal;Smad2* transheterozygous embryos exhibit anterior neural truncations, further suggesting that precise levels of Nodal signaling are required for neuroectoderm patterning (Nomura and Li, 1998). Upon activation, the receptor-activated Smads form a complex with Smad4 and translocate to the nucleus. Here, the Smad complex is recruited to Nodal target genes by its interaction with other DNA-binding proteins to regulate gene expression (Derynck et al., 1998; Whitman, 1998).

The first DNA-binding cofactor identified to interact with the Smad complex is the winged helix transcription factor, Foxh1 (also known as Fast1). Smad2 and Smad4 were shown to form a complex with Foxh1, and to bind to an activin-responsive element in the *Xenopus Mix.2* promoter (Chen et al., 1996; Chen et al., 1997). Cloning and mutational analysis of the *schmalspur* (*sur*) locus in zebrafish demonstrated that *sur* encodes Foxh1 and that it is required for the maintenance of Nodal signaling (Pogoda et al., 2000; Sirotkin et al., 2000). Consistent with this model, embryos lacking both maternal and zygotic *sur* (*MZsur*) show defects in axial mesoderm, although they do not exhibit the defects in endoderm and trunk mesoderm formation seen in embryos lacking the Nodal ligands Cyc and Sqt (Feldman et al., 1998). These data have led to the proposal that multiple transcription factors can mediate Nodal signaling in various developmental processes (Pogoda et al., 2000; Stemple, 2000).

Biochemical studies have shown that members of the Mix family of homeodomain proteins also function as transcriptional mediators of Nodal signaling (Germain et al., 2000), for example, by interacting with a Smad2/Smad4 complex upon Tgfβ signaling and binding the *goosecoid* (*gsc*) promoter. Mapping of the protein-protein interaction domain identified a common Smad interaction motif within a subgroup of the Mix family members, as well as in winged helix transcription factors, such as Foxh1 (Germain et al., 2000).

In zebrafish, the Mix gene *bonnie and clyde* (*bon*) functions downstream of Nodal signaling to regulate endoderm formation (Kikuchi et al., 2000). *bon* expression requires Nodal signaling as it is absent in $cyc^{-/-};sqt^{-/-}$ embryos (Alexander and Stainier, 1999). Additionally, misexpression of a constitutively active form of the type I Tgfβ receptor Tarama promotes ectopic *bon* expression (Alexander and Stainier, 1999). Furthermore, *bon* overexpression in $cyc^{-/-};sqt^{-/-}$ embryos can induce endodermal gene expression (Kikuchi et al., 2000). Finally, $bon^{-/-}$ embryos exhibit a severe reduction in the number of endodermal precursors, which indicates that *bon* plays a crucial role in endoderm formation. Here, we show that Bon also functions in precursors of the axial mesoderm to modulate anterior neural patterning. We further show that Bon functions cooperatively with the Nodal signaling components Sqt and Sur (Foxh1) to regulate this process. Expression analyses in single- and double-mutant embryos show a correlation between the severity of the neural patterning defects and the level of *dickkopf 1* (*dkk1*) expression. The defect in *dkk1* expression in the mutant embryos is part of an overall defect in dorsal mesendoderm gene expression.

Materials and methods

Zebrafish strains

Adult fish and embryos were maintained as described (Westerfield, 1994). Embryos were derived from mating of identified heterozyotes, homozygotes or transheterozygotes. The following mutant alleles were used: bon^{m425} (Stainier et al., 1996), sqt^{cz35} (Feldman et al., 1998) and sur^{m768} (Schier et al., 1996). Homozygous *sur* mutant adults were generated from $sur^{m768/+}$ intercrosses.

Microinjection

For restricted morpholino injection experiments, fluorescein-tagged morpholino oligonucleotides for *bon* (5′-GAT-TCG-CAT-TGT-GCT-GCT-GTC-CTT-C-3′) were dissolved in 5 mM HEPES, pH 7.6, and diluted to 2 ng/nl with 5 mM HEPES/10% Phenol Red. Rhodamine-dextran (10 kDa, 2.5%) was co-injected into some embryos in order to enhance the signal for localizing the morpholino. Antibody staining for the fluorescein-tagged morpholino indicated that the 10 kDa rhodamine-dextran co-localizes with the morpholino (data not shown). Single cells at the 32-cell stage were injected with 1 nl of a 2 ng/nl *bon* MO stock. Following injections, embryos were fixed for whole-mount in situ hybridization at the tailbud stage, or photographed using a Zeiss Axioplan microscope. Localization of the injected clone was visualized with a rhodamine filter, or an anti-fluorescein antibody following in situ hybridization. Briefly, embryos were treated with 100 mM glycine, pH 2.2, to inactivate alkaline phosphatase and washed with PBS-T (phosphate buffered saline + 0.1% Tween). Anti-fluorescein-alkaline phosphatase conjugated antibody (Boehringer Mannheim; 1:500) was incubated with embryos overnight at 4°C and detected with Fast Red (Sigma).

In situ hybridization

Whole-mount in situ hybridization was performed as described previously (Alexander et al., 1998). *dkk1* anti-sense probe was prepared as described by Hashimoto et al. (Hashimoto et al., 2000).

Genotyping

Whole-mount in situ hybridized embryos were genotyped by PCR using restriction polymorphisms for bon^{m425} and sur^{m768}, and agarose polymorphism for sqt^{cz35} mutant embryos, as described previously (Feldman et al., 1998; Kikuchi et al., 2000; Sirotkin et al., 2000). Genotyping was performed after in situ hybridization as follows. After photographing, each embryo was washed with 100% methanol and hydrated with several washes of PBS with 0.1% Tween-20. Genomic DNA was extracted by digestion overnight in 10 mM Tris, 1 mM EDTA, 0.1% NP40, 0.1% Tween-20, 50 μg proteinase K at 55°C.

Results

bon mutants exhibit a reduction in the anterior neuroectoderm

bon was initially identified as a mutation that causes cardia bifida, a condition in which the precardiac mesoderm fails to migrate to the midline and fuse (Stainier et al., 1996). At 28 hours post-fertilization (hpf), the cardia bifida phenotype is accompanied by pericardial edema (Fig. 1B; arrowhead). Previous

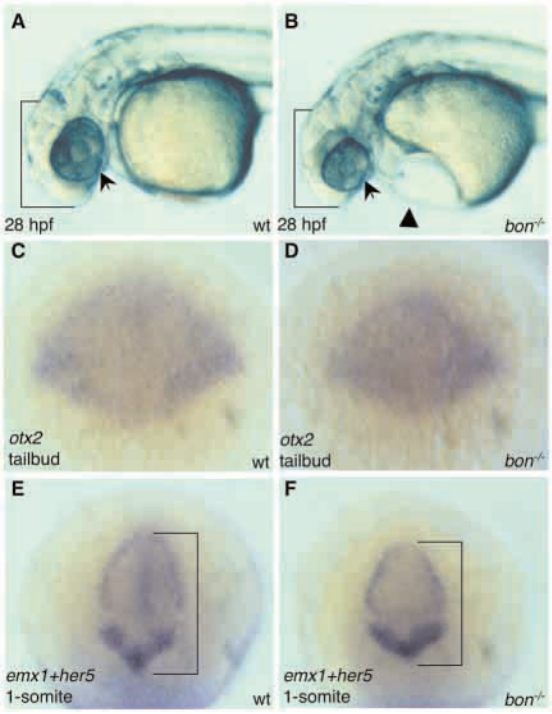

Fig. 1. *bon* mutant embryos exhibit anterior neural defects. (A,B) Lateral views (anterior to the left) of wild-type and *bon*$^{-/-}$ embryos at 28 hpf. Compared with wild-type siblings, *bon*$^{-/-}$ embryos show characteristic pericardial edema (arrowhead), as well as slightly smaller forebrain (brackets) and smaller eyes (arrows). (C,D) Dorsal views (anterior to the top) of *otx2* expression in the presumptive forebrain and midbrain regions of wild-type and *bon*$^{-/-}$ embryos at the tailbud stage. The *otx2* expression domain is smaller in *bon*$^{-/-}$ embryos. (E,F) Dorsal views (anterior to the top) of *emx1* and *her5* expression in wild-type and *bon*$^{-/-}$ embryos at the 1-somite stage. *emx1* expression marks the anterior edge of the neural plate and *her5* expression marks the midbrain-hindbrain boundary (MHB). The distance between the anterior edge of *emx1* expression and the posterior tip of *her5* expression (brackets) is reduced by about 10% in *bon*$^{-/-}$ embryos as compared with wild-type siblings. These anterior neural plate phenotypes (shown in D and F) segregated completely with the *bon* mutation, as assessed by genotyping.

characterization of *bon*$^{-/-}$ embryos has shown that the primary phenotype is a severe reduction in the number of endodermal precursors, and the likely cause of cardia bifida (Kikuchi et al., 2000). Closer inspection reveals that *bon*$^{-/-}$ embryos also exhibit reduced forebrain structures, with a reduction in eye size being most prominent (Fig. 1A,B; arrows). In order to assess whether this reduction reflects defects in neural patterning, we examined the expression of region-specific markers in the neural plate of early somite stage embryos. In *bon*$^{-/-}$ embryos, the *otx2* expression domain in the presumptive forebrain and midbrain regions (Mori et al., 1994) is approximately 10% smaller than wild type (Fig. 1C,D), suggesting that the anterior neural plate is reduced. Consistent with this result, double staining with *emx1*, a marker of the anterior boundary of the neural plate, and *her5*, a marker of the midbrain-hindbrain boundary (MHB), shows a reproducible and consistent reduction in the distance between the anterior edge of *emx1* expression and the posterior tip of *her5* expression in *bon*$^{-/-}$ embryos (Fig. 1E,F). These results suggest that *bon* functions not only in endoderm formation but also in neural patterning.

bon is required in the axial mesoderm for anterior neural development

bon is expressed in all mesendodermal progenitors prior to the onset of gastrulation (Alexander et al., 1999). The axial mesoderm is thought to promote neuroectodermal fates (reviewed by Harland and Gerhart, 1997), and the nonaxial mesoderm has been implicated in patterning the neuroectoderm (Woo and Fraser, 1997). To determine the mesendodermal derivative in which Bon function is required for neural patterning, we inhibited *bon* function in a tissue-specific manner by using morpholino antisense oligonucleotides (MO). Restriction of the *bon* MO was achieved by injecting it into a single cell at the 32-cell stage. The MO was conjugated to fluorescein to track its localization. In control experiments, *bon* MO injections at the one-cell stage phenocopy the *bon* mutation very specifically in more than 95% of the embryos (n>1000; data not shown).

To assess the anterior neural plate during the stages of neural patterning, MO-injected embryos were fixed and examined for *otx2* expression. Following in situ hybridization, we also performed anti-fluorescein antibody staining to determine the localization of the *bon* MO. Embryos with axial mesoderm restriction of the *bon* MO (n=25) showed a reduction in the *otx2* expression domain (Fig. 2A), whereas embryos with *bon* MO restriction in non-axial mesoderm (n=13) exhibited wild-type *otx2* expression (Fig. 2B,C).

In addition to in situ hybridization with *otx2*, individual MO-injected embryos were followed for morphological observations. At the effective MO concentration, the fluorescein-tag proved to be an ineffective lineage tracer in live embryos. Thus, as an additional lineage tracer, 10 kDa rhodamine-dextran was co-injected with the *bon* MO. Following antibody staining for fluorescein, we observed that the 10 kDa rhodamine-dextran co-localized with the *bon* MO in the co-injected embryos (data not shown), thus providing a reliable method to determine the localization of cells with reduced Bon function. Examples of tissue restriction are shown in Fig. 2D-F. As expected, embryos with *bon*-MO restriction in the neuroectoderm (n=2; Fig. 2F,F′), where *bon* is not expressed, were normal (Fig. 2F″). Consistent with the *otx2* expression data mentioned earlier, embryos with *bon*-MO restriction in the ventral mesoderm (n=5; Fig. 2E,E′) were also normal (Fig. 2E″). However, all embryos with *bon*-MO restriction in the axial mesoderm (n=27; Fig. 2D), derivatives of which populate the notochord (white arrowhead) and head mesenchyme (white arrow; Fig. 2D′), exhibited reduced forebrain structures, with a reduction in eye size being most prominent (Fig. 2D″; arrow), similar to the neural defects seen in *bon*$^{-/-}$ embryos. In addition, we excluded the endoderm as a tissue in which *bon* functions to modulate neural patterning because in embryos lacking all endoderm, such as *casanova* mutants, neural patterning is unaffected (data not shown). Together, these results indicate that Bon function is required in the axial mesoderm for neural patterning.

bon mutant embryos exhibit defects in axial mesodermal gene expression

To further analyze the requirement of the axial mesoderm during neural patterning, we examined the expression of the

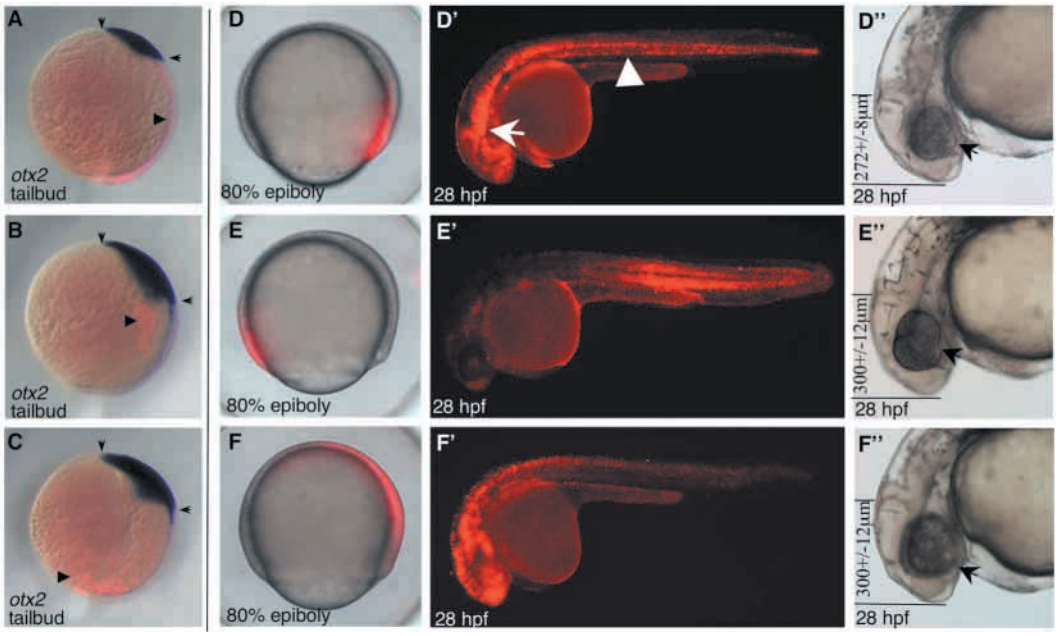

Fig. 2. *bon* is required in the axial mesoderm for neural patterning. Restricted injections of *bon* MO into a single cell at the 32-cell stage result in tissue specific knockdown of Bon function. Restriction of *bon* MO was determined by antibody staining for the fluorescein moiety conjugated to the MO (A-C) or by localization of co-injected 10 kDa rhodamine-dextran (D-F). (A-C) Lateral views (dorsal to the right) of *otx2* expression in *bon* MO-injected embryos at the tailbud stage. Embryos with restriction to the axial mesoderm (n=25; A), lateral mesoderm (n=3; B) and ventral mesoderm (n=10; C) are shown. Arrowheads point to the localization of the *bon* MOs, whereas arrows mark the area of *otx2* expression. Only embryos with *bon* MOs in the axial mesoderm showed a reduction of the *otx2*-expression domain (A). (D-F″) Lateral views of *bon* MO-injected embryos at 80% epiboly (D-F) and 28 hpf (D′-F″). The same embryos were followed and examined at 80% epiboly (D-F), 28 hpf for *bon*-MO restriction (D′-F′) and morphological defects in head formation (D″-F″). (D,D′,D″) Embryos with *bon* MOs in axial mesoderm, derivatives of which populate the notochord (white arrowhead) and head mesenchyme (white arrow), exhibited anterior defects, with a reduction in eye size (black arrow) being most prominent (n=27). Embryos with *bon* MO in non-axial tissues, such as ventral mesoderm (n=5; E) and neural ectoderm (n=2; F), exhibited no defects in neural development (E″,F″). Head size was determined on individual embryos by measuring the distance from the MHB to the tip of the telencephalon at 28 hpf. This distance was 272±8 μm in embryos with axial mesoderm restriction of the *bon* MO (n=27), and 300±12 μm in wild-type embryos or those with neuroectoderm or ventral mesoderm morpholino restriction (n=7).

anterior axial mesoderm marker *gsc* (Stachel et al., 1993) at several stages during gastrulation. At the shield stage, $bon^{-/-}$ embryos show *gsc* expression that is indistinguishable from that seen in wild-type embryos (Fig. 3A). At 90% epiboly, the *gsc* expression domain is reduced in $bon^{-/-}$ embryos (Fig. 3C), indicating a differentiation defect in the anterior axial mesoderm. The same progressive reduction in anterior axial mesoderm gene expression was also observed with *bmp4*. During gastrulation stages, *bmp4* is expressed ventrolaterally, as well as in a discrete domain of the anterior axial mesoderm (Hwang et al., 1997; Martinez-Barbera et al., 1997). This expression pattern allowed us to assess dorsoventral patterning as well as axial mesoderm formation. At 50% epiboly, wild-type and $bon^{-/-}$ embryos show indistinguishable *bmp4* expression ventrolaterally (Fig. 3D,G), indicating that dorsoventral patterning is not affected in $bon^{-/-}$ embryos. Dorsal *bmp4* expression also appears unaffected at this stage (Fig. 3D,G; arrowhead). At 90% epiboly, wild-type and $bon^{-/-}$ embryos show a wild-type pattern of ventrolateral *bmp4* expression (Fig. 3H,I), but the anterior axial mesoderm *bmp4* expression domain is dramatically reduced in $bon^{-/-}$ embryos (Fig. 3E,F,H,I; arrows). These data indicate that although the early induction of axial mesoderm occurs properly in $bon^{-/-}$ embryos, its subsequent differentiation is defective.

bon and *sqt* function in parallel to regulate neural patterning

In order to better understand the role of *bon* in neural patterning, we crossed $bon^{+/-}$ fish with fish heterozygous at other loci regulating axial mesoderm formation, and found a functional interaction between *bon* and the *nodal*-related gene *sqt*. Although $bon^{+/-}$ and $sqt^{+/-}$ embryos appear to have a wild-type phenotype, approximately 20% of $bon^{+/-};sqt^{+/-}$ embryos exhibit a cyclopic phenotype similar to that seen in $sqt^{-/-}$ embryos (Fig. 4C; arrow). In addition, whereas $bon^{-/-}$ embryos exhibit a slight reduction in forebrain structures (Fig. 2B; arrow), $bon^{-/-};sqt^{-/-}$ embryos exhibit a complete absence of forebrain, lacking telencephalic and diencephalic structures as well as eyes (arrow; Fig. 4D). Interestingly, this interaction was not found with the *nodal*-related gene *cyc*, further indicating that *sqt* and *cyc* play distinct roles in neural patterning. In addition, $MZsqt^{-/-}$ embryos do not exhibit as severe a defect as that seen in $bon^{-/-};sqt^{-/-}$ embryos (data not shown). Together, these data suggest that Bon and Sqt function in parallel to regulate neural patterning.

To assess the neural defects resulting from the loss of *bon* and *sqt* function, we analyzed the expression of region-specific markers in the neural plate of wild-type, $bon^{-/-}$, $sqt^{-/-}$ and $bon^{-/-};sqt^{-/-}$ embryos. At the 1-somite stage, *emx1* marks the anterior boundary of the neural plate, whereas *krox20* (*egr2b* – Zebrafish Information Network) marks rhombomeres 3 and 5 of the hindbrain (r3 and r5; Fig. 4E,I) (Oxtoby and Jowett, 1993). In $bon^{-/-}$ embryos, the distance between the anterior neural ridge (*emx1*) and the r5/r6 boundary, as well as the distance between r3 and r5 is reduced (Fig. 4F,J; brackets). In addition, the lateral borders of the neural plate (*emx1*) appear

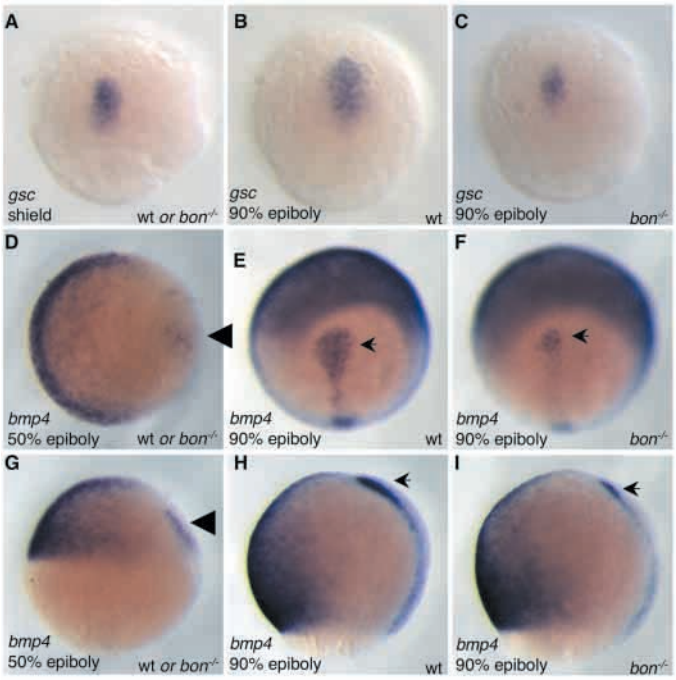

Fig. 3. *bon* mutant embryos exhibit defects in anterior axial mesoderm gene expression. Whole-mount in situ hybridization analyses at the shield stage (A), and at 50% (D,G) and 90% (B,C,E,F,H,I) epiboly, showing dorsal views (A-C; anterior to the top), animal pole views (D-F; D, dorsal to the right; E,F, anterior to the top) and lateral views (G-I; dorsal to the right). (A) At the shield stage, wild-type and $bon^{-/-}$ embryos show indistinguishable *gsc* expression. (B,C) At 90% epiboly, the *gsc* expression domain is reduced in $bon^{-/-}$ embryos as compared with wildtype. (D,G) At 50% epiboly, wild-type and $bon^{-/-}$ embryos show indistinguishable *bmp4* expression. Arrowheads point to the dorsal *bmp4* expression domain. (H,I) At 90% epiboly, wild-type and $bon^{-/-}$ embryos show a wild-type pattern of ventrolateral *bmp4* expression, but (E,F) the anterior axial mesoderm *bmp4* expression domain is dramatically reduced in $bon^{-/-}$ embryos (arrows). These phenotypes segregated completely with the *bon* mutation, as assessed by genotyping.

to be shifted medially (Fig. 4J; asterisks), further indicating a reduction in the neural plate. In $sqt^{-/-}$ and $bon^{-/-};sqt^{-/-}$ embryos, the reduction in the distance between the anterior edge of the neural plate and the r5/r6 boundary appears to be more dramatic (Fig. 4G,H). Additionally, r3 and r5, as marked by *krox20* staining, appear to be closer together in $bon^{-/-};sqt^{-/-}$ embryos (Fig. 4H,L). This apparent merging of r3 and r5, and the reduced distance between the anterior neural ridge and the r5/r6 boundary, indicates a reduction of neural tissue along the AP axis.

Anteriorly, the *emx1* expression domain spreads medially to cover the entire anterior ventral neural plate in $sqt^{-/-}$ and $bon^{-/-};sqt^{-/-}$ embryos (Fig. 4K,L). This expansion appears to be restricted to *emx1* expression, as *otx2* expression is reduced in $sqt^{-/-}$ and $bon^{-/-};sqt^{-/-}$ embryos (Fig. 4O,P). Consistent with this result, and with the morphological absence of eyes in $bon^{-/-};sqt^{-/-}$ embryos, the expression of *opl* (*zic1* – Zebrafish Information Network) and *rxb*, markers of the eye field, is dramatically reduced or absent in $bon^{-/-};sqt^{-/-}$ embryos (data not shown). Together, these data indicate that loss of *bon* and *sqt* function leads to synergistic defects in neural patterning.

bon and *sqt* function in parallel to regulate mesendodermal gene expression

AP patterning of the neuroectoderm is regulated by posteriorizing signals and their antagonists (reviewed by Yamaguchi, 2001). Recent evidence points to the Wnt signaling pathway as a key regulator of AP patterning, with Wnt8 as a posteriorizing signal and the Wnt antagonist Dkk1 as promoting anterior neural fates (Glinka et al., 1998; Erter et al., 2001). The neural patterning defects in $bon^{-/-}$, $sqt^{-/-}$ and $bon^{-/-};sqt^{-/-}$ embryos were reminiscent of defects caused by an excess of Wnt signaling (Kim et al., 2000; Erter et al., 2001). Therefore, we examined the expression of *dkk1* in $bon^{-/-}$, $sqt^{-/-}$ and $bon^{-/-};sqt^{-/-}$ embryos and found that defects in *dkk1* expression correlated with the severity of the neural patterning defects observed in these mutant embryos. At 50% epiboly, *dkk1* expression is observed in all marginal blastomeres (Fig. 5A) (Hashimoto et al., 2000; Shinya et al., 2000). In $bon^{-/-}$ embryos, there is a dorsal gap in *dkk1* expression (Fig. 5B). This dorsal gap appears more extensive in $sqt^{-/-}$ and $bon^{+/-};sqt^{+/-}$embryos (Fig. 5C). In $bon^{-/-};sqt^{-/-}$ embryos, *dkk1* expression is seen only in the ventral half of the margin (Fig. 5D). At 70% epiboly, *dkk1* is expressed in cells of the prechordal plate (PCP; Fig. 5E) (Hashimoto et al., 2000; Shinya et al., 2000). Consistent with $bon^{-/-}$ embryos exhibiting defects in anterior axial mesoderm gene expression, the *dkk1*-expressing cells appear to coalesce aberrantly in these mutants (Fig. 5F). In $sqt^{-/-}$ and $bon^{+/-};sqt^{+/-}$ embryos, *dkk1* expression in the PCP is dramatically reduced (Fig. 5G), reflecting a defect in anterior axial mesoderm formation. This reduction is enhanced in $bon^{-/-};sqt^{-/-}$ embryos, where *dkk1* expression appears to be completely absent in the PCP region (Fig. 5H). These data suggest that the defects in *dkk1* expression may be responsible, at least in part, for the neural patterning defects. In order to test this hypothesis, we overexpressed *dkk1* in $bon^{-/-}$ embryos and observed an enlargement of the forebrain and eyes, suppressing the anterior neural deficiency (data not shown). However, the cardia bifida phenotype was not rescued, suggesting that *dkk1* functions in neural patterning but not in endoderm development.

In addition to defects in *dkk1* expression, we found that $bon^{-/-};sqt^{-/-}$ embryos have defects in dorsal mesendoderm gene expression. In wild-type and $bon^{-/-}$ embryos at 50% epiboly, *ntl* is expressed around the margin of the embryo (Fig. 5I,J). In $sqt^{-/-}$ or $bon^{+/-};sqt^{+/-}$ embryos, *ntl* expression appears reduced (Fig. 5K), and, in $bon^{-/-};sqt^{-/-}$ embryos, it is absent from the dorsal half of the margin (Fig. 5L), suggesting that the formation of dorsal mesoderm is defective in $bon^{-/-};sqt^{-/-}$ embryos. This reduction in dorsal mesendoderm gene expression in $bon^{-/-};sqt^{-/-}$ embryos was also observed with other markers, such as *wnt8* (data not shown). Thus, in $bon^{-/-};sqt^{-/-}$ embryos, the lack of *dkk1* expression from dorsal mesendoderm may reflect an overall deficit in dorsal mesendoderm gene expression, which suggests that *bon* and *sqt* function in parallel to regulate dorsal mesendoderm formation as well as neural patterning.

bon interacts with *sur* to regulate neural patterning and mesendodermal gene expression

The genetic interaction between *bon* and *sqt* suggested that these two genes function in parallel to regulate neural patterning. However, molecular epistasis analyses have indicated that *bon* expression is dependent on Nodal signaling, which places *bon*

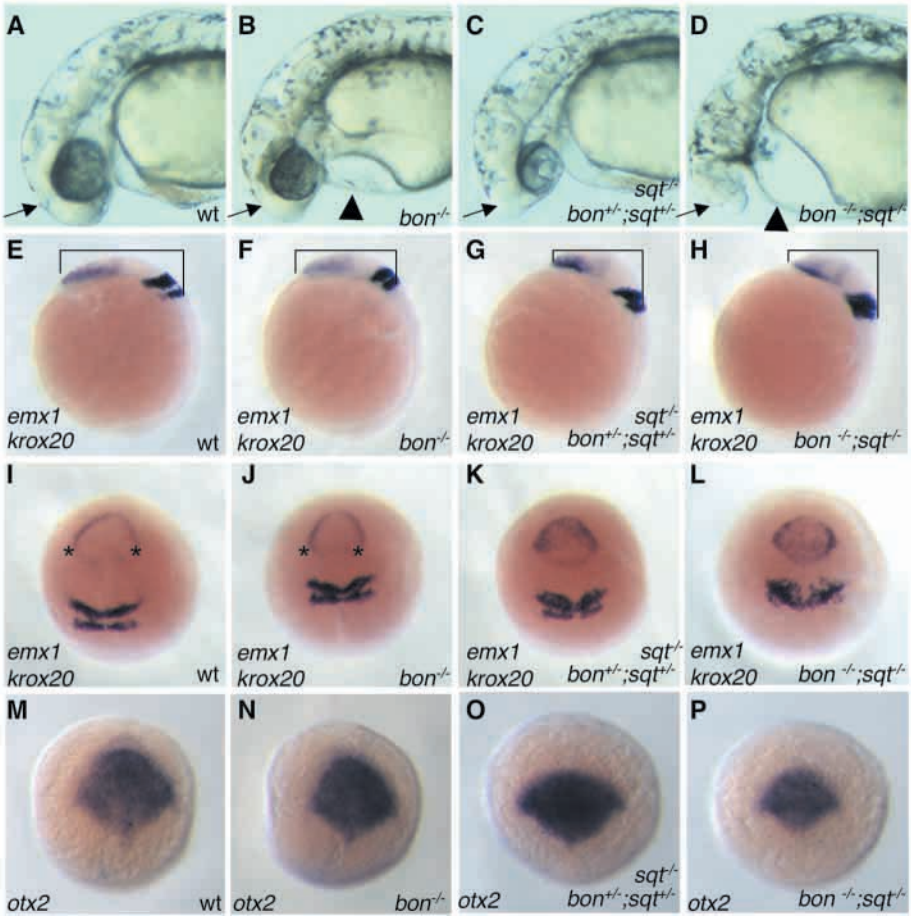

Fig. 4. *bon* interacts with *sqt* to regulate neural patterning. Nomarski images at 30 hpf (A-D) and whole-mount in situ hybridization analyses at 1-somite (E-L) and tailbud stages (M-P), showing lateral (A-H; A-D, anterior to the left; E-H, dorsal to the right) and animal pole views (I-P; anterior to the top). Compared with wild-type siblings (A), *bon*$^{-/-}$ embryos (B) have severe pericardial edema (arrowhead) and smaller forebrain structures (arrow), *sqt*$^{-/-}$ and some *bon*$^{+/-}$;*sqt*$^{+/-}$ embryos (C) are cyclopic, and *bon*$^{-/-}$;*sqt*$^{-/-}$ embryos (D) have severe pericardial edema (arrowhead) and lack anterior structures (arrow). (E-L) Whole-mount in situ hybridization analyses with *emx1* and *krox20* at the 1-somite stage. At the 1-somite stage, *emx1* marks the anterior boundary of the neural plate and *krox20* rhombomeres 3 and 5 (r3 and r5). In *bon*$^{-/-}$ embryos (F,J), the distance between the anterior neural ridge (*emx1*) and the r5/r6 boundary is reduced (brackets), and the distance between r3 and r5 is also reduced. The lateral borders of the *emx1*-expression domain (asterisks) are also shifted medially in *bon*$^{-/-}$ embryos (J). In *sqt*$^{-/-}$ or *bon*$^{+/-}$;*sqt*$^{+/-}$ (G) and *bon*$^{-/-}$;*sqt*$^{-/-}$ (H) embryos, the reduction in the distance between the anterior edge of *emx1* expression and the r5/r6 boundary (brackets) is more pronounced. In addition, instead of outlining the neural plate, *emx1* expression spreads medially throughout the entire area of the anterior ventral neural plate in *sqt*$^{-/-}$ or *bon*$^{+/-}$;*sqt*$^{+/-}$ (K) and *bon*$^{-/-}$;*sqt*$^{-/-}$ (L) embryos. This expansion does not appear to be an expansion of anterior neural fates as *otx2*-expression domains are reduced in *sqt*$^{-/-}$ or *bon*$^{+/-}$;*sqt*$^{+/-}$ (O) and *bon*$^{-/-}$;*sqt*$^{-/-}$ (P) embryos, when compared with either wild-type (M) or *bon*$^{-/-}$ embryos (N). These neural patterning defects segregated completely with the respective *bon*, *sqt* and *bon;sqt* mutations, as assessed by genotyping.

downstream of *sqt* (Alexander et al., 1999). Thus, additional signal(s) must function upstream of *bon*, and additional Nodal transcriptional mediator(s) must function downstream of *sqt*. The *foxh1* gene mutant locus *sur* was a good candidate to be an additional Nodal transcriptional mediator in neural patterning due to its role in axis formation (Pogoda et al., 2000; Sirotkin et al., 2000). Therefore, we asked whether *bon*$^{-/-}$;*sur*$^{-/-}$ embryos exhibit neural patterning defects. Although *bon*$^{-/-}$ embryos exhibit a slight reduction in anterior neural structures (Fig.1B and Fig. 4B; arrow) and *sur*$^{-/-}$ embryos exhibit mild cyclopia (Pogoda et al., 2000; Sirotkin et al., 2000), *bon*$^{-/-}$;*sur*$^{-/-}$ embryos exhibit a dramatic reduction of forebrain structures, with the most severally affected embryos exhibiting an absence of telencephalic and diencephalic structures, as well as eyes (Fig. 6B; arrow). Interestingly, *bon*$^{-/-}$;*sur*$^{+/-}$ embryos also exhibited anterior truncations at a low percentage (1.8%, *n*=340) when they originated from *bon*$^{+/-}$;*sur*$^{+/-}$ females but not from *bon*$^{+/-}$;*sur*$^{+/-}$ males, indicating that a reduction in maternal Sur (Foxh1) can enhance the *bon* neural phenotype.

The loss of anterior structures in *bon*$^{-/-}$;*sur*$^{-/-}$ embryos was reminiscent of the *bon*$^{-/-}$;*sqt*$^{-/-}$ phenotype (Fig. 4D); thus, we used the same region-specific neural markers that were employed in the *bon*$^{-/-}$;*sqt*$^{-/-}$ analyses to assess neural patterning in *bon*$^{-/-}$;*sur*$^{-/-}$ embryos. At the tailbud stage, *bon*$^{-/-}$;*sur*$^{-/-}$ embryos exhibit a dramatic reduction in the distance between the anterior edge of *emx1* expression and the r5/r6 boundary (Fig. 6F; bracket). In addition, the rhombomeres r3 and r5 appear closer together (Fig. 6J). The similarity in neural patterning defects between *bon*$^{-/-}$;*sur*$^{-/-}$ and *bon*$^{-/-}$;*sqt*$^{-/-}$ embryos indicates that Sur (Foxh1) may be the additional Nodal transcriptional mediator functioning downstream of Sqt and in parallel to Bon in neural patterning (Fig. 7).

To further analyze the similarity in neural patterning defects between *bon*$^{-/-}$;*sur*$^{-/-}$ and *bon*$^{-/-}$;*sqt*$^{-/-}$ embryos, we examined *dkk1* expression in *bon*$^{-/-}$;*sur*$^{-/-}$ embryos. We found that at 50% and 70% epiboly, *bon*$^{-/-}$;*sur*$^{-/-}$ embryos exhibit a loss of *dkk1* expression (Fig. 6C,D,G,H) similar to that seen in *bon*$^{-/-}$;*sqt*$^{-/-}$ embryos (Fig. 5C). Further, we found that expression of *ntl* is also absent from the dorsal side of *bon*$^{-/-}$;*sur*$^{-/-}$ embryos (Fig. 6K,L), which suggests that the formation of dorsal mesendoderm is defective in *bon*$^{-/-}$;*sur*$^{-/-}$ embryos. Altogether, these data indicate that Bon and Sur (Foxh1) function in parallel to regulate dorsal mesendoderm gene expression and neural patterning.

Discussion

In this study, we show that the Mix homeodomain gene *bon* is

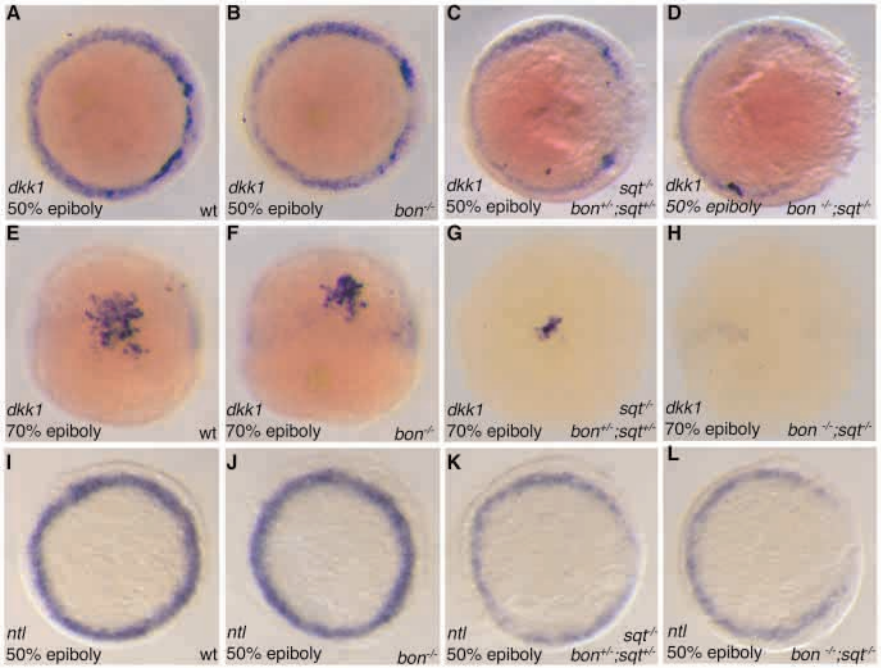

Fig. 5. *bon* and *sqt* function in parallel to regulate mesendodermal gene expression. Whole-mount in situ hybridization analyses of *dkk1* (A-H) and *ntl* (I-L) expression, showing animal pole (A-D,I-L; dorsal to the right) and dorsal views (E-H; anterior to the top). At 50% epiboly, *dkk1* expression is seen in all marginal blastomeres in wild-type embryos (A). In $bon^{-/-}$ embryos, *dkk1* expression exhibits a slight dorsal gap (B). In $sqt^{-/-}$ or $bon^{+/-};sqt^{+/-}$ embryos, this dorsal gap appears more extensive (C). In $bon^{-/-};sqt^{-/-}$ embryos, *dkk1* expression is seen only in the ventral half of the margin (D). At 70% epiboly, *dkk1* is expressed in cells of the PCP in wild-type embryos (E). In $bon^{-/-}$ embryos, the *dkk1*-expressing cells appear to coalesce aberrantly (F). In $sqt^{-/-}$ or $bon^{+/-};sqt^{+/-}$ embryos, *dkk1* expression in the PCP is dramatically reduced (G). In $bon^{-/-};sqt^{-/-}$ embryos, *dkk1* expression appears to be completely absent (H). At 50% epiboly in wild-type and $bon^{-/-}$ embryos, *ntl* is expressed around the margin of the embryo (I,J). In $sqt^{-/-}$ embryos, *ntl* expression appears reduced around the entire margin (K). In $bon^{-/-};sqt^{-/-}$ embryos, *ntl* expression appears reduced around the margin and is absent from the dorsal side (L). The *dkk1* and *ntl* expression defects segregated completely with the respective *bon*, *sqt* and *bon;sqt* mutations, as assessed by genotyping.

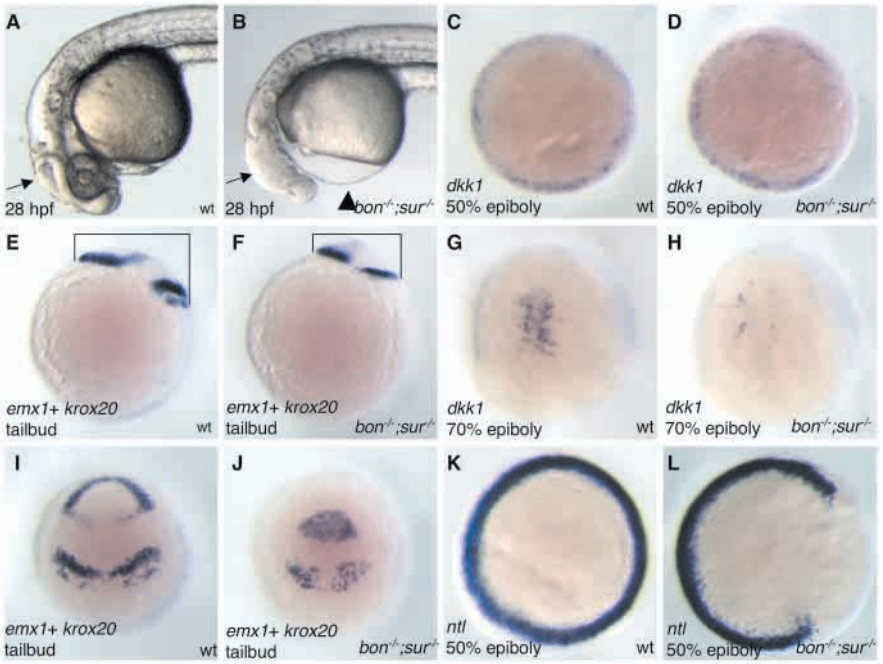

Fig. 6. *bon* interacts with *sur* (*foxh1*) to regulate mesendodermal gene expression and neural patterning. Nomarski images at 28 hpf (A,B) and whole-mount in situ hybridization analyses at 50% (C,D,K,L) and 70% epiboly (G,H), and at the tailbud stage (E,F,I,J). A,B and E,F are lateral views (A,B, anterior to the left; E,F, dorsal to the right); C,D and I-L are animal pole views (C,D,K,L, dorsal to the right; I,J, anterior to the top); and G,H are dorsal views (anterior to the top). Compared with wild-type siblings (A), $bon^{-/-};sur^{-/-}$ embryos (B) have severe pericardial edema (arrowhead) and lack anterior structures (arrow). (E,F,I,J) Whole-mount in situ hybridization analyses with *emx1* and *krox20* at the tailbud stage. At the tailbud stage, the distance between the anterior neural ridge (*emx1*) and the r5/r6 boundary (brackets) is dramatically reduced in $bon^{-/-};sur^{-/-}$ embryos (F), similar to that observed in $bon^{-/-};sqt^{-/-}$ embryos (Fig. 4h). In addition, *emx1* expression is also expanded medially in $bon^{-/-};sur^{-/-}$ embryos (J). At 50% epiboly, *dkk1* expression is seen in all marginal blastomeres in wild-type embryos (C), whereas in $bon^{-/-};sur^{-/-}$ embryos it exhibits a dorsal gap (D). At 70% epiboly, *dkk1* is clearly expressed in cells of the PCP of wild-type embryos (G), whereas in $bon^{-/-};sur^{-/-}$ embryos it is dramatically reduced (H). At 50% epiboly, *ntl* is expressed around the margin of the embryo (K), whereas in $bon^{-/-};sur^{-/-}$ embryos it is absent from the dorsal side (L). These neural patterning and mesendodermal gene expression defects segregated completely with the *bon;sur* mutations, as assessed by genotyping.

required in the axial mesoderm to regulate neural patterning. Our results indicate that the severity of the neural patterning defects in $bon^{-/-}$ embryos correlates with the degree of reduction in *dkk1* expression in the dorsal mesendoderm and, subsequently, the anterior axial mesoderm. Genetic interactions between *bon* and the components of the Nodal signaling pathway, *sqt* and *sur* (*foxh1*), reveal a complex network that mediates Nodal signaling in neural patterning. First, the genetic interaction between *bon* and *sqt* suggests that the relationship between *bon* and *sqt* is not strictly linear as previously suggested by molecular epistasis

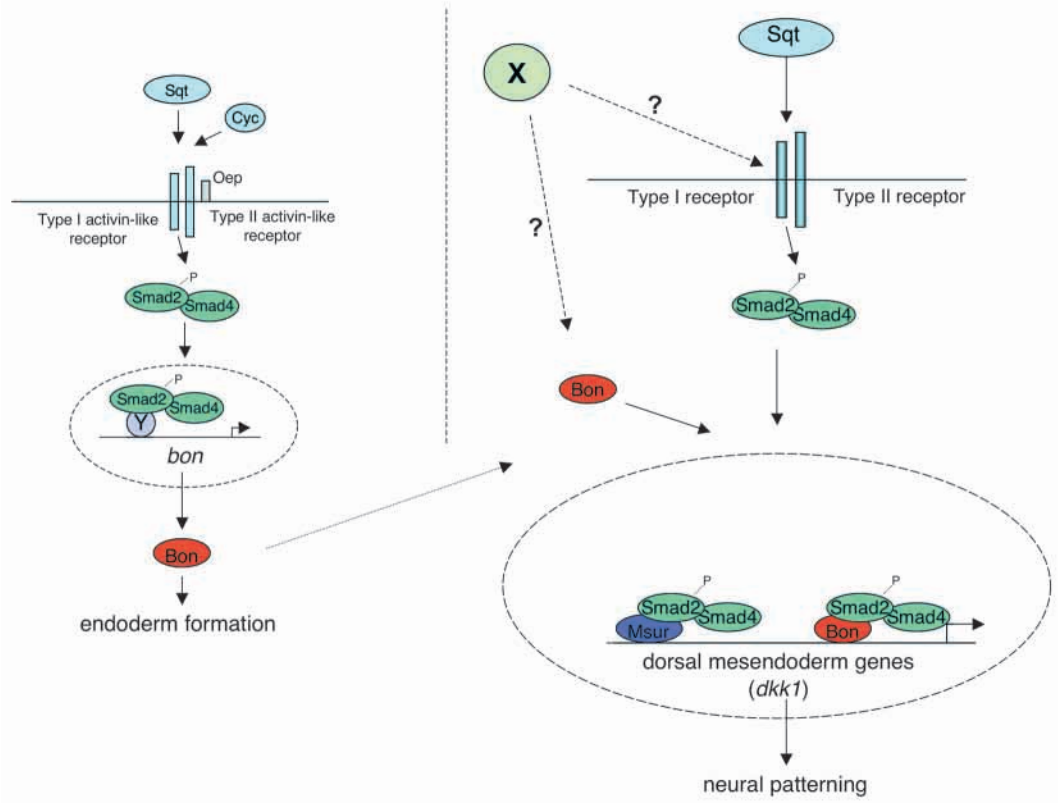

Fig. 7. A model for the genetic network of Nodal signaling. Combining our results with biochemical (Germain et al., 2000) and molecular epistasis data (Alexander et al., 1999), a model emerges in which the Nodal signal provided by Sqt is transduced by a Smad2/Smad4 complex. In endoderm formation, Bon functions downstream of Nodal signaling. The identity of the transcriptional mediator (Y) of Nodal signaling regulating *bon* expression is not known. The genetic interactions between *bon;sqt* and *bon;sur* indicate that Bon also functions in parallel to Sqt and Sur (Foxh1) to regulate mesendodermal target genes, such as *dkk1* and *ntl*. These genes in turn regulate neural patterning. The more than additive defects seen in $bon^{-/-};sqt^{-/-}$ and $bon^{-/-};sur^{-/-}$ embryos, which are not seen in $MZsqt^{-/-}$ embryos, suggest that an additional, as yet unidentified, factor (X) may be involved in this network, regulating Bon function at least. Whether factor X regulates Bon function through Smad activation remains to be determined.

studies (Alexander et al., 1999; Kikuchi et al., 2000). Second, the *bon;sur* interaction demonstrates that these two transcriptional factor genes play overlapping functions in neural patterning. Finally, expression studies indicate that Bon, Sqt and Sur (Foxh1) function to regulate dorsal mesendoderm genes, such as *ntl* and *dkk1*, the latter playing an important role in neural patterning (Glinka et al., 1998; Hashimoto et al., 2000; Mukhopadhyay et al., 2001; Shinya et al., 2000).

A role for *bon* in neural patterning

Genetic and embryological analyses indicate that Mix genes are potent inducers of mesodermal and endodermal gene expression. Ectopic expression of *Mix.1*, *Milk*, *Mixer*, *Bix1*, *mezzo* and *bon* leads to the expression of mesodermal and endodermal genes (Henry and Melton, 1998; Lemaire et al., 1998; Alexander et al., 1999; Latinkic and Smith, 1999; Poulain and Lepage; 2002). Additionally, a genetic lesion in the zebrafish Mix gene *bon* leads to a reduction in endodermal precursors (Kikuchi et al., 2000). Our data point to an essential role for Bon in the axial mesoderm for neural patterning. We found that a reduction in Bon function in the axial mesoderm caused by restricted MO injection is associated with anterior neural defects. In addition, $bon^{-/-}$ embryos display defects in axial mesoderm gene expression. Furthermore, based on the expression pattern of *bon* in mesendodermal progenitors before involution, we favor a model in which Bon regulates the transcription of neural patterning genes that are expressed in mesendodermal precursors. The finding that *dkk1* expression is absent from the dorsal side of $bon^{-/-}$ embryos is consistent with this model. It is interesting to note that studies in *Xenopus* had hinted at a role for *Mixer* in head formation and *Dkk1* expression (Henry and Melton, 1998).

Nodal signaling regulates neural patterning through transcriptional regulation of members of the Wnt signaling pathway

Recent findings have revealed that the spatial variation in the level of Wnt signal plays a crucial role in the AP patterning of the neuroectoderm (reviewed by Yamaguchi, 2001; Erter et al., 2001; Kudoh et al., 2002). Extensive evidence from genetic and overexpression studies points to the importance of Wnt antagonism for anterior neural patterning. Specifically, *Dkk1* mouse mutant embryos lack head structures anterior to the midbrain, whereas overexpression of *dkk1* in amphibians and zebrafish embryos leads to enlarged heads (Glinka et al., 1998; Hashimoto et al., 2000; Mukhopadhyay et al., 2001; Shinya et al., 2000). Conversely, ectopic expression of *wnt8* suppresses anterior fates, whereas a deficiency in the *wnt8* locus or a reduction of Wnt8 caused by MO injection in zebrafish embryos leads to a loss of posterior neural fates (Erter et al., 2001; Lekven et al., 2001). Our data indicate that the precise level of Wnt signaling required for neural patterning is transcriptionally controlled by Nodal signaling as well as by Bon and Sur (Foxh1).

Bon and Sqt function in parallel to regulate neural patterning

Overexpression and mutant analyses have indicated that Bon functions exclusively downstream of Nodal signaling in

endoderm formation (Alexander et al., 1999; Kikuchi et al., 2000). However the synergistic neural patterning defects seen in *bon*$^{-/-}$;*sqt*$^{-/-}$ embryos indicate that Bon also functions in parallel to Sqt signaling. Biochemical analyses indicate that a subset of Mix homeodomain proteins, as well as winged-helix transcription factors, physically interact with the Smad2/Smad4 complex through a conserved motif in their C terminus (Germain et al., 2000). This Smad interaction motif is present in Bon and Sur (Foxh1) (Pogoda et al., 2000; Randall et al., 2002), raising the possibility that Bon and/or Sur (Foxh1) can interact with the Smad2/Smad4 complex, upon Sqt activation of the Nodal pathway, to activate downstream targets. The loss of *dkk1* expression in *bon*$^{-/-}$;*sqt*$^{-/-}$ and *bon*$^{-/-}$;*sur*$^{-/-}$ embryos indicates that *dkk1* is one of the genes regulated in this manner. Whether Bon and Sur (Foxh1) bind directly to the *dkk1* promoter needs to be investigated.

In addition, we also found defects in *wnt8* expression at the margin of *bon*$^{-/-}$;*sqt*$^{-/-}$ embryos suggesting that the neural patterning defect in these double-mutant embryos may not be solely due to an expansion of Wnt signaling. We do observe a shortening of the body axis in *bon*$^{-/-}$;*sqt*$^{-/-}$ and *bon*$^{-/-}$;*sur*$^{-/-}$ embryos, which may lead to a misplacement of neural organizing centers, such as the anterior neural boundary cells and the MHB (reviewed by Liu and Joyner, 2001; Houart et al., 1998), which would further affect AP patterning of the neural plate (see Fig. 4E-H, Fig. 6E-F).

Model of genetic network of transcriptional mediators of Nodal signaling

By combining our results with biochemical (Germain et al., 2000) and molecular epistasis data (Alexander et al., 1999), a model emerges in which the Nodal signal provided by Sqt is transduced by a complex of Smad2/Smad4 that is recruited to specific target genes by either Bon or Sur (Foxh1; Fig. 7). These two transcriptional mediators of Nodal signaling have unique functions during the formation of endoderm and axial mesoderm but have overlapping activities in neural patterning. The genetic interactions between *bon;sqt* and *bon;sur* indicate that Bon functions in parallel to Sqt and Sur (Foxh1) to regulate the expression of mesendodermal genes, such as *dkk1*, which in turn is required for neural patterning.

In endoderm formation, Bon functions downstream of Nodal signaling in an Oep-dependent fashion (Alexander et al., 1999; Kikuchi et al., 2000). *bon* expression is unaffected in *MZsur*$^{-/-}$ embryos (data not shown), suggesting that an additional Smad-binding transcription factor is involved in regulating *bon* expression (Fig. 7; factor Y*)*. A possible candidate for this activity could be the Mix-like transcription factor, Mezzo that was shown to function downstream of Nodal signaling. However, *bon* expression is probably not regulated by Mezzo as Mezzo lacks a Smad interaction motif and *mezzo* MO-injected embryos do not exhibit endoderm defects (Poulain and Lepage, 2002). Thus, we propose that an additional, as yet unidentified, Smad-binding transcription factor (Y) is involved in the initiation of *bon* expression.

Once *bon* expression is initiated, our model places Bon and Sur (Foxh1) as the two transcriptional mediators of Sqt signaling in neural patterning. However, it should be re-emphasized that *MZsqt*$^{-/-}$ embryos exhibit a less severe neural patterning defect than that seen in either *bon*$^{-/-}$;*sqt*$^{-/-}$ or *bon*$^{-/-}$;*sur*$^{-/-}$ embryos, which indicates that Sqt is not the sole signal regulating Bon transcriptional activity. Thus, an additional factor (X) may function upstream of Bon and in parallel to Sqt in neural patterning. In this model, factor X could correspond to Cyc, as it has been suggested that the ventrolateral mesoderm, which requires Nodal signaling for its formation, can provide a secondary posteriorizing signal to the neural plate (Erter et al., 2001; Feldman et al., 2000; Woo and Fraser, 1997). The neural defect seen in *bon*$^{-/-}$;*sqt*$^{-/-}$ and *bon*$^{-/-}$;*sur*$^{-/-}$ embryos, but not in *cyc*$^{-/-}$;*sqt*$^{-/-}$ embryos, may be caused by the presence of ventrolateral mesoderm and its posteriorizing effect on the neural plate. Further studies should reveal how the various Nodal ligands, as well as other signals, regulate neural patterning, either directly, or through their regulation of mesendodermal gene expression.

We thank Pia Aanstad, Elke A. Ober and Nick Osborne for comments on the manuscript and helpful discussions. L.A.T. was supported by a National Science Foundation Predoctoral fellowship. This work was supported in part by grants from the NIH (DK 58181) and the Packard Foundation to D.Y.R.S.

References

Alexander, J. and Stainier, D. Y. R. (1999). A molecular pathway leading to endoderm formation in zebrafish. *Curr. Biol*. **9**, 1147-1157.

Alexander, J., Stainier, D. Y. and Yelon, D. (1998). Screening mosaic F1 females for mutations affecting zebrafish heart induction and patterning. *Dev. Genet.* **22**, 288-299.

Brennan, J., Lu, C. C., Norris, D. P., Rodriguez, T. A., Beddington, R. S. P. and Robertson, E. J. (2001). Nodal signaling in the epiblast patterns the early mouse embryo. *Nature* **411**, 965-969.

Chen, X., Rubock, M. J. and Whitman, M. (1996). A transcriptional partner for Mad proteins in TGF-β signaling. *Nature* **383**, 691-696.

Chen, X., Weisberg, E., Fridmacher, V., Watanabe, M., Naco, G. and Whitman, M. (1997). Smad4 and Fast-1 in the assembly of activin-responsive factor. *Nature* **389**, 85-89.

Conlon, F. L., Lyons, K. M., Takaesu, N., Barth, K. S., Kispert, A., Hermann, B. and Robertson, E. J. (1994). A primary requirement for nodal in the formation and maintenance of the primitive streak in the mouse. *Development* **120**, 1919-1928.

Derynck, R., Zhang, Y. and Feng, X. H. (1998). Smads: transcriptional activators of TGF-β responses. *Cell* **95**, 737-740.

Erter, C. E., Wilm, T. P., Basler, N., Wright, C. V. E. and Solnica-Krezel, L. (2001). Wnt8 is required in lateral mesendodermal precursors for neural posteriorization in vivo. *Development* **128**, 3571-3583.

Feldman, B., Gates, M. A., Egan, E. S., Dougan, S. T., Rennebeck, G., Sirotkin, H. I., Schier, A. F. and Talbot, W. S. (1998). Zebrafish organizer development and germ-layer formation require nodal-related signals. *Nature* **395**, 181-185.

Feldman, B., Dougan, S. T., Schier, A. F. and Talbot, W. S. (2000). Nodal-related signals establish mesendodermal fate and trunk neural identity in zebrafish. *Curr. Biol*. **10**, 531-534.

Germain, S., Howell, M., Esslemont, G. M. and Hill, C. S. (2000). Homeodomain and wing-helix transcription factors recruit activated Smads to distinct promoter elements via a common Smad interaction motif. *Genes Dev.* **14**, 435-451.

Glinka, A., Wu, W., Delius, H., Monaghan, A. P., Blumenstock, C. and Niehrs, C. (1998). Dickkopf1 is a member of a new family of secreted proteins and functions in head induction. *Nature* **391**, 357-362.

Gritsman, K., Zhang, J., Cheng, S., Heckscher, E., Talbot, W. S. and Schier, A. F. (1999). The EGF-CFC protein one-eye pinhead is essential for nodal signaling. *Cell* **97**, 121-132.

Harland, R. and Gerhart, J. (1997). Formation and function of Spemann's organizer. *Annu. Rev. Cell Dev. Biol*. **13**, 611-667.

Hashimoto, H., Itoh, M., Yamanaka, Y., Yamashita, S., Shimizu, T., Solnica-Krezel, L., Hibi, M. and Hirano, T. (2000). Zebrafish *Dkk1* functions in forebrain specification and axial mesendoderm formation. *Dev. Biol*. **217**, 138-152.

Henry, G. L. and Melton, D. A. (1998). *Mixer*, a homeobox gene required for endoderm development. *Science* **281**, 91-96.

Houart, C., Westerfield, M. and Wilson, S. W. (1998). A small population of anterior cells patterns the forebrain during zebrafish gastrulation. *Nature* **391**, 788-792.

Hwang, S. P., Tsou, M. F., Lin, Y. C. and Liu, C. H. (1997). The zebrafish *BMP4* gene: sequence analysis and expression pattern during embryonic development. *DNA Cell Biol.* **8**, 1003-1011.

Kikuchi, Y., Trinh, L. A., Reiter, J. F., Alexander, J., Yelon, D. and Stainier, D. Y. R. (2000). The zebrafish *bonnie and clyde* gene encodes a Mix family homeodomain protein that regulates the generation of endodermal precursors. *Genes Dev.* **14**, 1279-1289.

Kim, C., Oda, T., Itoh, M., Jiang, D., Artinger, K. B., Chandrasekharappa, S. C., Driever, W. and Chitnis, A. B. (2000). Repressor activity of *Headless/Tcf3* is essential for vertebrate head formation. *Nature* **407**, 913-916.

Kudoh, T., Wilson, S. W. and Dawid, I. B. (2002). Distinct roles for Fgf, Wnt and retinoic acid in posteriorizing the neural ectoderm. *Development* **129**, 4335-4346.

Latinkic, B. W. and Smith, J. C. (1999). Goosecoid and mix.1 repress Brachyury expression and are required for head formation in Xenopus. *Development* **26**, 769-779.

Lekven, A. C., Thorpe, C. J., Waxman, J. S. and Moon, R. T. (2001). Zebrafish *wnt8* encodes two Wnt8 proteins on a bicistronic transcript and is required for mesoderm and neuroectoderm patterning. *Dev. Cell* **1**, 103-114.

Lemaire, P., Darras, S., Caillol, D. and Kodjabachian, L. (1998). A role for the vegetally expressed *Xenopus* gene Mix.1 in endoderm formation and in the restriction of mesoderm to the marginal zone. *Development* **25**, 2371-2380.

Liu, A. and Joyner, A. L. (2001). Early anterior/posterior patterning of the midbrain and cerebellum. *Annu. Rev. Neurosci.* **24**, 869-896.

Lowe, L. A., Yamada, S. and Kuehn, M. R. (2001). Genetic dissection of *nodal* function in patterning the mouse embryo. *Development* **128**, 1831-1843.

Martinez-Barbera, J. P., Toresson, H., Da Rocha, S. and Krauss, S. (1997). Cloning and expression of three members of the zebrafish BMP family: Bmp2a, Bmp2b and Bmp4. *Gene* **198**, 53-59.

Mori, H., Miyazaki, Y., Morita, T., Nitta, H. and Mishina, M. (1994). Different spatio-temporal expressions of three Otx homeoprotein transcripts during zebrafish embryogenesis. *Brain Res. Mol. Brain Res.* **27**, 221-231.

Mukhopadhyay, M., Shtrom, S., Rodriguez-Esteban, C., Chen, L., Tsukui, T., Gomer, L., Dorward, D. W., Glinka, A., Grinberg, A., Huang, S., Niehrs, C., Belmonte, J. and Westphal, H. (2001). *Dickkopf1* is required for embryonic head induction and limb morphogenesis in the mouse. *Dev. Cell* **1**, 423-434.

Nomura, M. and Li, E. (1998). Smad2 role in mesoderm formation, left-right patterning and craniofacial development. *Nature* **393**, 786-790.

Osada, S. I. and Wright, C. V. (1999). *Xenopus* nodal-related signaling is essential for mesendodermal pattering during early embryogenesis. *Development* **126**, 3229-3240.

Oxtoby, E. and Jowett, T. (1993). Cloning of the zebrafish *krox-20* gene (*krx-20*) and its expression during hindbrain development. *Nucl. Acids Res.* **21**, 1087-1095.

Pogoda, H., Solnica-Krezel, L., Driever, W. and Meyer, D. (2000). The zebrafish forkhead transcription factor FoxHI/Fast1 is a modulator of Nodal signaling required for organizer formation. *Curr. Biol.* **10**, 1041-1049.

Poulain, M. and Lepage, T. (2002). Mezzo, a paired-like homeobox protein is an immediate target of Nodal signaling and regulates endoderm specification in zebrafish. *Development* **21**, 4901-4914.

Randall, R. A., Germain, S., Inman, G. J., Bates, P. A. and Hill, C. S. (2002). Different Smad2 partners bind a common hydrophobic pocket in Smad2 via a defined proline-rich motif. *EMBO J.* **21**, 145-156.

Sampath, K., Rubinstein, A. L., Cheng, A. M. S., Liang, J. O., Fekany, K., Solnica-Krezel, L., Korzh, V., Halpern, M. E. and Wright, C. V. E. (1998). Induction of the zebrafish ventral brain and floorplate requires cyclops/nodal signaling. *Nature* **395**, 185-189.

Schier, A. F. and Shen, M. M. (1999). Nodal signaling in vertebrate development. *Nature* **403**, 385-389.

Schier, A. F., Neuhauss, S. C. F., Harvey, M., Malicki, J., Solnica-Krezel, L., Stainier, D. Y., Zwartkruis, F., Abdelilah, S., Stemple, D. L., Rangini, Z. et al. (1996). Mutations affecting the development of the embryonic zebrafish brain. *Development* **23**, 165-178.

Shinya, M., Eschbach, C., Clark, M., Lehrach, H. and Seiki, M. F. (2000). Zebrafish *Dkk1*, induced by the pre-MBT Wnt signaling, is secreted from the prechordal plate and patterns the anterior neural plate. *Mech. Dev.* **98**, 3-17.

Sirotkin, H. I., Dougan, S. T., Schier, A. F. and Talbot, W. S. (2000). *bozozok* and *squint* act in parallel to specify dorsal mesoderm and anterior neuroectoderm in zebrafish. *Development* **127**, 2583-2592.

Sirotkin, H. I., Gates, M. A., Kelly, P. D., Schier, A. F. and Talbot, W. S. (2000). *fast1* is required for the development of dorsal axial structures in zebrafish. *Curr. Biol.* **10**, 1051-1054.

Stachel, S. E., Grunwald, D. J. and Myers, P. Z. (1993). Lithium perturbation and *goosecoid* expression identify a dorsal specification pathway in the pregastrula zebrafish. *Development* **117**, 261-274.

Stainier, D. Y., Fouquet, B., Chen, J. N., Warren, K. S., Weinstein, B. M., Meiler, S. E., Mohideen, M. A., Neuhauss, S. C., Solnica-Drezel, L., Schier, A. F. et al. (1996). Mutations affecting the formation and function of the cardiovascular system in the zebrafish embryo. *Development* **123**, 285-292.

Stemple, D. L. (2000) Vertebrate development: the fast track to Nodal signaling. *Curr. Biol.* **10**, R843-R846.

Thisse, B., Wright, C. V. E. and Thisse, C. (2000). Activin-and Nodal-related factors control antero-posterior patterning of the zebrafish embryo. *Nature* **403**, 425-428.

Tremblay, K. D., Hoodless, P. A., Bikoff, E. K. and Robertson, E. J. (2002). Formation of the definitive endoderm in mouse is a Smad2-dependent process. *Development* **27**, 3079-3090.

Waldrip, W. R., Bikoff, E. K., Hoodless, P. A., Wrana, J. L. and Robertson, E. J. (1998). Smad2 signaling in extraembryonic tissues determines anterior-posterior polarity of the early mouse embryo. *Cell* **92**, 797-808.

Weinsten, M., Yang, X., Li, C., Xu, X., Gota, J. and Deng, C. X. (1998). Failure of egg cylinder elongation and mesoderm induction in mouse embryos lacking the tumor suppressor smad2. *Proc. Natl. Acad. Sci. USA* **95**, 9378-9383.

Westerfield, M. (1994). The zebrafish book. Eugene, OR: University of Oregon Press.

Whitman, M. M. (1998). Smads and early developmental signaling by the TGFbeta superfamily. *Genes Dev.* **12**, 2445-2462.

Whitman, M. (2001). Nodal signaling in early vertebrate embryos: themes and variations. *Dev. Cell* **1**, 605-617.

Woo, K. and Fraser, S. E. (1997). Specification of the Zebrafish nervous system by nonaxial signals. *Science* **277**, 254-257.

Yamaguchi, T. P. (2001). Heads and tails: Wnts and anterior-posterior patterning. *Curr. Biol*. **11**, R713-R724.

Zhou, X., Sasaki, H., Lowe, L., Hogan, B. L. and Kuehn, M. R. (1993). *Nodal* is a novel TGF-β-like gene expressed in the mouse node during gastrulation. *Nature* **361**, 543-547.